Cell, Vol. 99, 577–587, December 10, 1999, Copyright ©1999 by Cell Press

The DNA Double-Strand Break Repair Gene *hMRE11* Is Mutated in Individuals with an Ataxia-Telangiectasia-like Disorder

Grant S. Stewart,* Richard S. Maser,† Tanja Stankovic,* Debra A. Bressan,† Mark I. Kaplan,† Nikolaas G. J. Jaspers,‡ Anja Raams,‡ Philip J. Byrd,* John H. J. Petrini,†§ and A. Malcolm R. Taylor*§

*The University of Birmingham CRC Institute for Cancer Studies
The Medical School
Edgbaston, Birmingham, B15 2TT
United Kingdom

†University of Wisconsin Medical School
Madison, Wisconsin 53706

‡Department of Cell Biology and Genetics
Erasmus University
3000 DR Rotterdam
The Netherlands

Summary

We show that hypomorphic mutations in *hMRE11*, but not in *ATM*, are present in certain individuals with an ataxia-telangiectasia-like disorder (ATLD). The cellular features resulting from these *hMRE11* mutations are similar to those seen in A-T as well as NBS and include hypersensitivity to ionizing radiation, radioresistant DNA synthesis, and abrogation of ATM-dependent events, such as the activation of Jun kinase following exposure to γ irradiation. Although the mutant hMre11 proteins retain some ability to interact with hRad50 and Nbs1, formation of ionizing radiation-induced hMre11 and Nbs1 foci was absent in *hMRE11* mutant cells. These data demonstrate that ATM and the hMre11/hRad50/Nbs1 protein complex act in the same DNA damage response pathway and link hMre11 to the complex pathology of A-T.

Introduction

Description of the genetic defects underlying the chromosomal instability syndromes ataxia-telangiectasia (A-T)(Savitsky et al., 1995) and Nijmegen breakage syndrome (NBS)(Carney et al., 1998; Varon et al., 1998) has provided important insight regarding the mammalian DNA damage response. Both A-T and NBS exhibit hypersensitivity to ionizing radiation, immunodeficiency, and an increased predisposition to the development of malignancies (reviewed by Shiloh, 1997). These phenotypic outcomes indicate that ATM and Nbs1, the gene products deficient in A-T and NBS, play an important role in maintaining genomic integrity in the face of intrinsic as well as extrinsic DNA damage. A clear biochemical link between double-strand break (DSB) repair and mammalian cellular responses to DNA damage was uncovered by the observation that Nbs1 functions in a complex with the highly conserved DSB repair proteins hMre11 and hRad50 (Carney et al., 1998).

§To whom correspondence should be addressed (e-mail: a.m.r.taylor@bham.ac.uk [A. M. R. T.], jpetrini@facstaff.wisc.edu [J. H. J. P.]).

The hMre11/hRad50/Nbs1 complex has been proposed to act as a sensor of DNA damage. Nelms et al. (1998) showed that upon exposure to ionizing radiation the hMre11/hRad50/Nbs1 complex becomes rapidly associated with the DNA DSBs and remains at these sites until the damage is repaired. Loss of functional Nbs1 in NBS patients prevents the formation of the radiation-induced hMre11/hRad50 nuclear foci (IRIF) (Carney et al., 1998). Similarly, the formation of the hMre11/hRad50/Nbs1 radiation-induced foci is abnormal in A-T cells, but the defect observed is less severe than in NBS cells (Maser et al., 1997). Since Nbs1 and ATM deficiencies abrogate specific DNA damage-dependent cell cycle checkpoints, the association of the hMre11/hRad50/Nbs1 complex with DSBs suggests that the DNA damage recognition functions of the complex are linked to the signal transduction pathway(s) required to activate ATM-dependent cell cycle checkpoints.

Interestingly, certain phenotypic features of the yeast mutants affecting the *S. cerevisiae* Mre11/Rad50/Xrs2 protein complex are reminiscent of both A-T and NBS; in addition to recombinational DNA repair deficiency, these mutants exhibit genomic instability in the form of increased allelic recombination, increased frequency of chromosome loss, and sensitivity to DNA damaging agents (Ajimura et al., 1993; Petrini et al., 1997; Bressan et al., 1998).

In the present study, we have identified two families clinically diagnosed with A-T that have mutations in the human *hMRE11* gene. Consistent with the clinical outcome of these mutations, cells established from the affected individuals within the two families exhibit many of the features characteristic of both A-T and NBS: chromosomal instability, increased sensitivity to ionizing radiation, defective induction of stress-activated signal transduction pathways, and radioresistant DNA synthesis (RDS). These data strengthen the molecular connection between DSB recognition by the hMre11/hRad50/Nbs1 protein complex and the ability of the cell to activate the DNA damage response pathway controlled by ATM.

Results

ATLD Patients Contain Mutations in the *hMRE11* Gene

We encountered two families in which the affected individuals presented with many clinical features of A-T, especially progressive cerebellar degeneration. Although none of the affected individuals from either family exhibited ocular telangiectasia, their clinical presentations were otherwise consistent with the diagnosis of A-T. Previously, we reported the increased cellular and chromosomal radiosensitivity of two cousins (ATLD1, a 25-year-old woman, and ATLD2, a 20-year-old man) in family 1 (Hernandez et al., 1993). Approximately 8% of peripheral lymphocytes carried translocations including t(7;14)(p15;q32) and t(7;14)(q35;q11) seen in A-T patients. Chromosomal radiosensitivity in lymphocytes

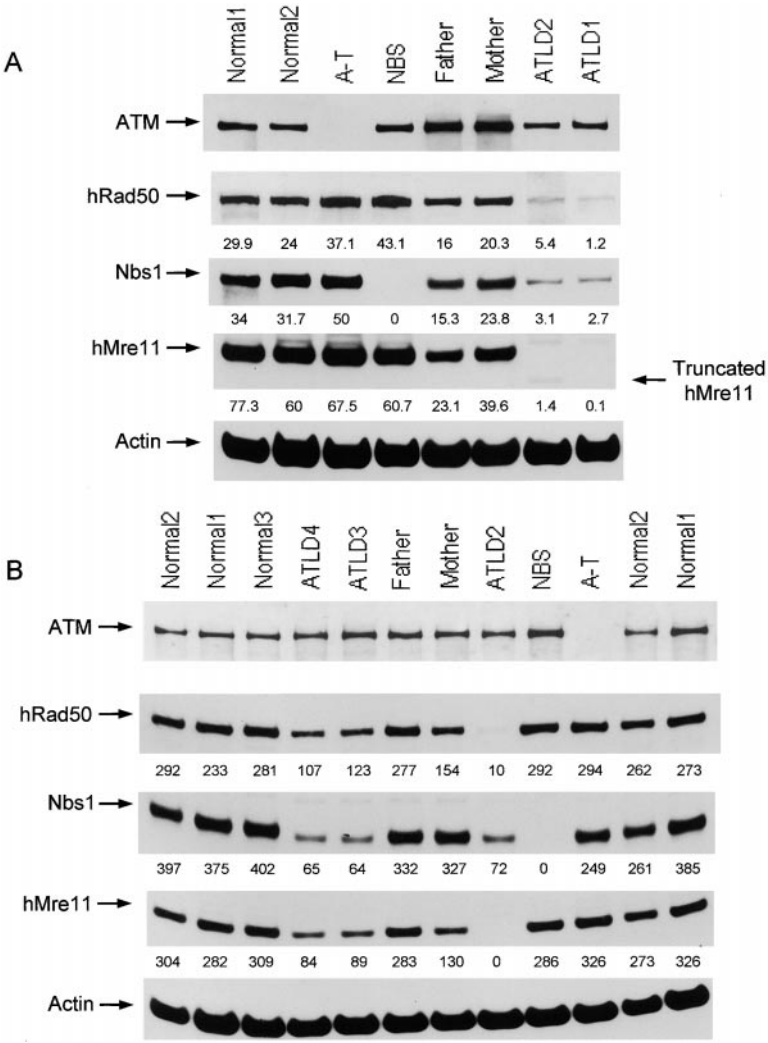

Figure 1. Alteration in Protein Levels of Full-Length hMre11, hRad50, and Nbs1 in ATLD Cells

Whole-cell extracts were made from LCLs derived from patients and normal individuals and fractionated by SDS polyacrylamide gel electrophoresis. Western blot analysis was performed using antisera directed against the ATM, hMre11, hRad50, and Nbs1 proteins. The Western blot was additionally probed for actin to standardize for protein loading. Protein:actin ratios are indicated.

(A) Whole-cell extracts from patients ATLD1 and ATLD2 in family 1 (father = father of ATLD2; mother = mother of ATLD1).

(B) Whole-cell extracts from ATLD3, ATLD4, and parents.

was increased to the level seen in classical A-T patients (Hernandez et al., 1993). Using haplotype analysis, we previously observed that patients ATLD1 and ATLD2 had different haplotypes in the region of the *ATM* gene, consistent with the A-T in this family not being due to an *ATM* mutation (Hernandez et al., 1993; patients are indicated in this publication as II-7 and II-8, respectively). Further haplotyping (data not shown), using $(C\text{-}A)_n$ markers, confirmed our original observation of different haplotypes in ATLD1 and ATLD2. In addition, we searched for *ATM* mutations in these two cousins by restriction endonuclease fingerprinting (REF) and also by sequencing selected parts of the cDNA, but no *ATM* mutation was found (data not shown).

In family 2, two brothers (ATLD3 and ATLD4) had clinical features of ataxia-telangiectasia (Klein et al., 1996). They also showed an increased level of chromosome translocations [1% of cells with t(7;14)(q35;q11)] and an increased chromosomal radiosensitivity intermediate between A-T and normal (indicated as patients 53, II-1, and II-2 in Taylor et al., 1996a) but not as high as ATLD1 and ATLD2. The parents were unrelated. In this family, both brothers did share the same haplotypes in the region of the *ATM* gene, which would be consistent with a diagnosis of A-T. We searched for *ATM* mutations in these two brothers by REF, but no *ATM* mutations were found (McConville et al., 1996). Consistent with the failure to detect mutations in *ATM*, normal ATM protein levels were present in all four patients from both families (Figure 1). Hence, we have designated this disorder ATLD, for ataxia-telangiectasia-like disorder.

Given the absence of ATM deficiency and the similarity between NBS and A-T at the cellular level, we then examined the status of the hMre11, hRad50, and Nbs1 proteins in ATLD cells. In ATLD1 and ATLD2, there was total loss of full-length hMre11 expression, with truncated hMre11 being observed in patient ATLD2 but not confirmed in ATLD1 on a Western blot (although truncated hMre11 could be coimmunoprecipitated from both ATLD1 and 2 cells by Nbs1 antibody; see below). In addition, there was a marked decrease in the levels of hRad50 and Nbs1 in these cells. In the parents, hMre11 levels were reduced compared with normal cells (Figure 1A).

In the patients ATLD3 and ATLD4, reduced levels of hMre11, hRad50, and Nbs1 were observed, but none of these proteins was present in a truncated form. Cells from the mother, but not the father, of these boys also

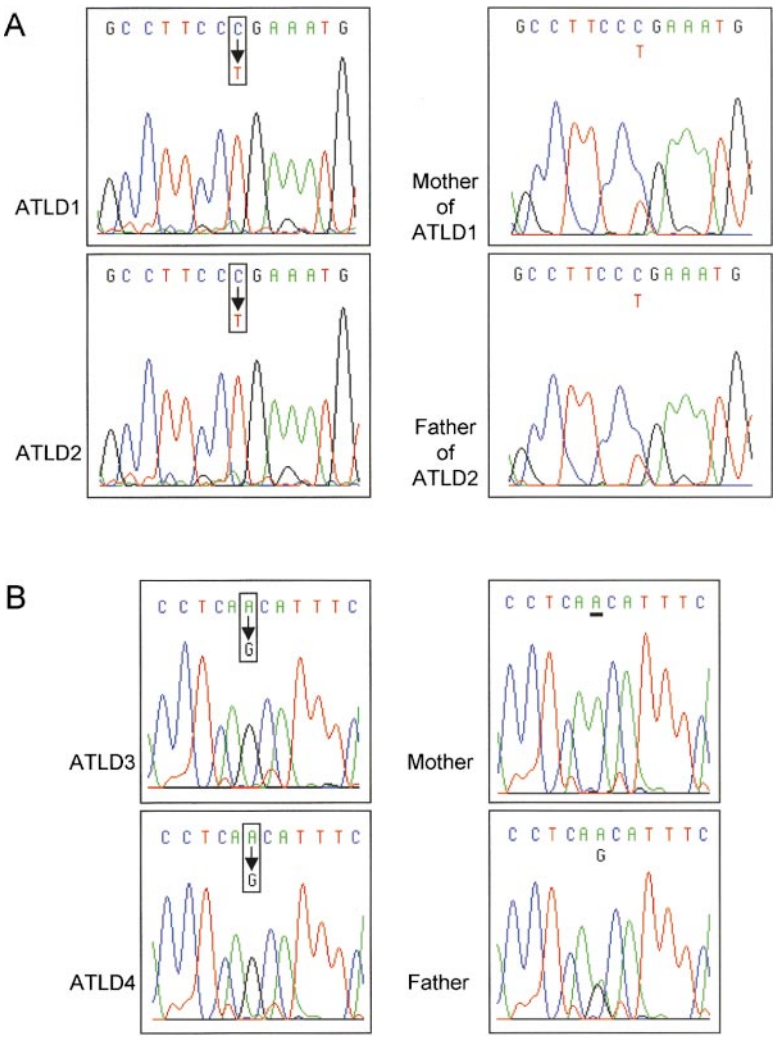

Figure 2. Identification of *hMRE11* Mutations in Two ATLD Families

(A) Family 1. Patients ATLD1 and ATLD2 are cousins and are homozygous for a C→T transition at nucleotide 1897, creating an in-frame stop codon. The mother of ATLD1 and father of ATLD2 are siblings and carry the same mutation. The other parents in this consanguineous family are also carriers of this mutation (data not shown).

(B) Family 2. Patients ATLD3 and ATLD4 are siblings and carry an A→G missense mutation at nt350, resulting in an N→S amino acid change. This mutation is paternal in origin, and both A and G can be seen at this position in the paternal sequence. The mother appears to be homozygous for the normal base A at this position. No A peak, coincident with the G peak from the father, is apparent in the *hMRE11* cDNA sequence in the two affected offspring. This suggested that the affected offspring have inherited a maternal allele that is either deleted, not transcribed, or is aberrantly processed with the effect that the mother is hemizygous at this position.

showed reduced hMre11 levels (Figure 1B). As previously observed, cells from a classical A-T patient contained hMre11, hRad50, and Nbs1 at normal levels, and only Nbs1 was lost in NBS cells as judged by Western blotting (Maser et al., 1997; Carney et al., 1998) (Figure 1). Therefore, NBS, A-T, and the ATLD disorder can be distinguished from each other by the levels of hMre11, hRad50, and Nbs1.

Since alteration in the levels of hMre11 was common to both families, the sequence of the *hMRE11* gene from the four ATLD patients was determined. In patients ATLD1 and ATLD2, a C→T change at nt1897 was detected. This change, CGA→TGA, resulted in a 633 R→STOP, prematurely truncating the hMre11 protein as we observed. Both patients from family 1 are homozygous for this mutation. Both parents of ATLD1 are cousins, as are the parents of ATLD2. In addition, the mother of ATLD1 and father of ATLD2 are siblings. Three of the four parents were shown to be heterozygous for the same mutation (Figure 2A) (the father of ATLD1 was deceased).

DNA sequence analysis of ATLD3 and ATLD4 *hMRE11* cDNA revealed one missense mutation, 350 A→G, resulting in a 117 N→S amino acid change, which was paternal in origin. Neither ATLD3 nor ATLD4 expressed a *hMRE11* allele with wild-type sequence at position 350 (Figure 2B), suggesting a deletion of this part of the maternal allele, possibly at the level of aberrant splicing or a mutation affecting transcription regulation. No maternally derived mutation was detected by DNA sequence analysis, suggesting that the mother of this family is heterozygous for a null *hMRE11* mutation. Western blotting showed reduced hMre11 levels in maternally derived cells, consistent with this interpretation (Figure 1B).

Phenotypic Characterisation of ATLD Cells

The clinical presentations of both ATLD families were very similar to that seen in A-T. To examine whether this similarity extended to the respective cellular phenotypes, several aspects of the DNA damage response were tested in cells established from ATLD patients. Cellular radiosensitivity was measured by colony forming ability of γ irradiated skin fibroblasts. In ATLD3 and ATLD4, colony forming ability was intermediate between classical A-T and normal controls, whereas survival in ATLD2 was nearer that of cells from classical A-T (Figure 3A). Healthy ATLD1 fibroblasts were unavailable, but

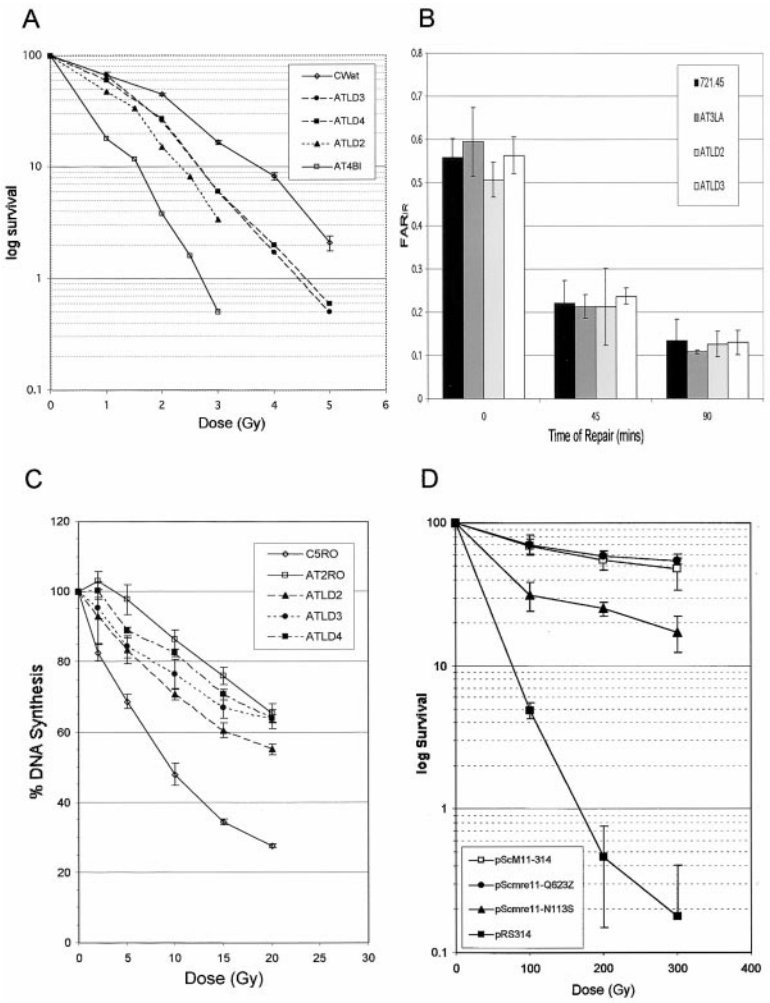

Figure 3. Radiosensitivity in *hMRE11* Mutants

(A) ATLD skin fibroblasts are unusually radiosensitive. Colony forming assay indicating survival levels of cells from ATLD2, 3, and 4 cells compared with normal (Cwat) and a A-T patient (AT4BI) following γ ray exposures up to 5 Gy. The values are means of two experiments for ATLD cells and three experiments for AT4BI and Cwat.

(B) ATLD LCLs are DSB repair proficient. Bar chart indicating the FAR_{IR} for normal (721.45), ATLD2, ATLD3, and A-T (AT3LA) LCLs after a dose of 50 Gy and repair for the indicated times. Data are obtained from four (721.45 cells) or two (ATLD2, ATLD3, AT3LA cells) independent experiments, and plugs were run on two gels. Error bars indicate the standard deviation among all gel runs.

(C) ATLD cells show radioresistant DNA synthesis (RDS). Levels of RDS in both A-T cells (AT2RO) and also ATLD cells from patients ATLD2, ATLD3, and ATLD4, compared with normal (C5RO) following γ ray doses of up to 20 Gy. Values are the means of three experiments.

(D) Radiation sensitivity of *Scmre11* mutants is also seen. Haploid *Scmre11*Δ strain JPY180 was transformed with a native promoter-driven *ScMRE11*, *Scmre11-Q623Z* (equivalent mutation to that in ATLD1 and 2), or *Scmre11*-N113S (equivalent mutation to that in ATLD3 and 4) expression constructs or the empty vector pRS314 (*Scmre11*Δ). Cultures of JPY180 transformants were γ irradiated at the doses indicated. Values plotted represent the average of three independent experiments. Error bars represent standard deviation.

previous work has shown them to have survival levels similar to A-T cells (Hernandez et al., 1993), consistent with the fact that ATLD1 and ATLD2 harbor the same *hMRE11* allele.

A-T cells are not grossly defective at DSB repair (Jorgensen and Shiloh, 1996). However, the evidence in *S. cerevisiae* demonstrating that ScMre11 functions in DSB repair prompted us to investigate whether the IR sensitivity of ATLD cells was attributable to DSB repair deficiency. We performed pulsed-field gel electrophoresis on cells that were irradiated at 50 Gy and allowed to repair for 0, 45, or 90 min. The fraction of DNA that migrates into the gel in an irradiation-dependent manner (FAR_{ir}) correlates with the number of DSBs (Ager and Dewey, 1990). We found that neither the initial level of radiation-induced DSBs nor the kinetics of DSB repair differed significantly among control, ATLD2, ATLD3, and A-T lymphoblastoid cell lines (LCLs) ($p > 0.1$ for 0 min, $p > 0.5$ for 45 and 90 min)(Figure 3B). Under the conditions used, DSB repair defects are readily observed in the DNA-PK-deficient cell line, MO59J (data not shown) (Lees-Miller et al., 1995). Therefore, the IR sensitivity observed in the ATLD patients does not appear to result from gross deficiency in DSB repair.

Failure to suppress DNA synthesis upon treatment with ionizing radiation is a hallmark of cells established from A-T as well as NBS patients (Shiloh, 1997). We assessed the ability of ATLD cells to effect this mode of DNA damage-dependent cell cycle regulation. The suppression of DNA inhibition in fibroblasts from ATLD patients 2, 3, and 4 is somewhat less pronounced than in the reference A-T cell strain, AT2RO, in which the RDS response is identical to that of other A-T strains (Jaspers et al., 1982) (Figure 3C). However, none of the ATLD cells suppressed DNA synthesis to the same level as the wild-type control. In this regard, ATLD2, 3, and 4 resemble the RDS phenotype seen in NBS fibroblasts (Kleijer and N. G. J. J., unpublished data). Hence, both *hMRE11* alleles expressed in the ATLD families impair the activation of the S phase DNA damage checkpoint.

Two aspects of the A-T phenotype that appear to be distinct from S phase checkpoint defects are the failure of A-T cells to effect the c-Abl-mediated induction of stress-activated protein kinases (SAPKs) (c-Jun N-terminal kinases) (Shafman et al., 1995) and the failure of these cells to stabilize p53 in response to γ irradiation. We examined ATLD cells for their ability to activate JNK following ionizing radiation (IR) treatment. JNK activity present in whole-cell extracts from IR-treated LCLs was tested with a GST-jun substrate. Whereas JNK activity

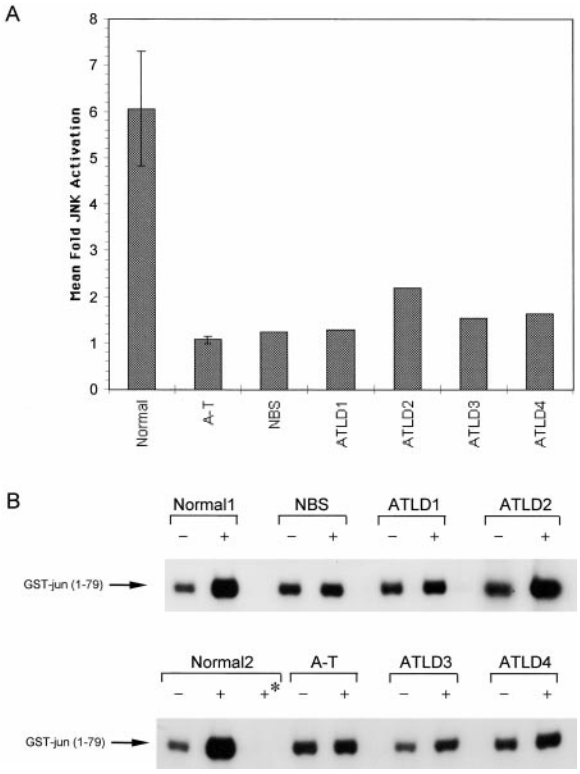

Figure 4. Jun Kinase Activity in ATLD Cells, A-T, and NBS Cells Is Deficient Compared with Normal

(A) Bar chart showing that the mean fold increase in Jun kinase, induced by ionizing radiation, as measured by the phosphorylation of GST-c-Jun, in normal, A-T, NBS, and ATLD cells (normal and A-T are both the mean of nine experiments; the remainders are each a mean of two experiments).

(B) Autoradiograph showing phosphorylation of GST-c-Jun (1–79) substrate. The various cell lines indicated were either mock irradiated (−) or irradiated with 20 Gy γ rays (+). JNK was immunoprecipitated and used to phosphorylate GST-c-Jun (1–79) substrate. The asterisk denotes immunoprecipitates from irradiated normal cells using nonspecific rabbit IgG. Band density was quantified by densitometry to give the fold increase in the chart above.

in normal cells was stimulated approximately 6-fold by IR, this activity was essentially unaffected by IR treatment of NBS and ATLD cells (Figure 4). Consistent with previous analyses, IR-induced activation of JNK in A-T cells was not observed in this assay (Shafman et al., 1995).

In contrast, both the timing and the magnitude of the p53 response in ATLD2, 3, and 4 fell within the range defined by two control LCLs. An NBS cell line was also tested and found to have a similarly normal p53 response (Figure 5). Although the p53 response in ATLD1 was indistinguishable from A-T cells, the *p53* gene was sequenced and found to be wild type. The basis of this finding is unclear, but it appears to be an idiosyncrasy of ATLD1 rather than a property of the ATLD1 *hMRE11* allele. We infer that the induced p53 was transcriptionally active in these cell lines, since normal MDM2 induction was observed in ATLD2, 3, and 4, as well as in the NBS line (data not shown). Hence, although the cellular phenotypes of ATLD and A-T are very similar, they can be distinguished from one another on the basis of the p53 response as well as by the severity of the RDS phenotype.

ATLD Mutations in *ScMRE11*

Given the high degree of conservation between the human and yeast Mre11 proteins, we reasoned that modeling the ATLD mutations in the *ScMRE11* gene would provide insight into the severity of those alleles. We derived *Scmre11*-Q623Z- (ATLD1/2) and *Scmre11*-N113S- (ATLD3/4) expressing strains and examined them with respect to mitotic function (sensitivity to IR) and meiotic function (spore viability).

The C-terminal truncation allele, *Scmre11*-Q623Z, exhibited wild-type resistance to IR, consistent with previous studies demonstrating that deletion of the C terminus of ScMre11 has very little impact on Mre11 function(s) in mitotic cells (Nairz and Klein, 1997; Furuse et al., 1998; Usui et al., 1998). In contrast, the N-terminal missense mutation, *Scmre11*-N113S, conferred significant IR sensitivity (Figure 3D).

In meiotic cells, both ATLD mutants exhibited defects in spore viability, suggestive of impaired meiotic recombination. The *Scmre11*-Q623Z truncation mutant was unable to produce viable spores (0 viable out of 100 total spores), and the *Scmre11*-N113S mutant produced viable spores at a reduced frequency relative to wild type (37% relative to 55%, respectively). Hence, it is clear that both mutations impair Mre11 function.

Interactions of hMre11, hRad50, and Nbs1 in Cells from ATLD Patients

To assess whether the mutant hMre11 proteins expressed in ATLD impair complex formation, we examined the integrity of the hMre11/hRad50/Nbs1 protein complex in ATLD cells. Neither truncation of the hMre11 protein at amino acid 633 (R→STOP) nor the presence of the missense mutation N→S at amino acid 117 entirely abolished the Nbs1 interaction with hMre11. Nbs1 monoclonal antibody efficiently immunoprecipitated hMre11 from normal cell extracts, whereas substantially reduced amounts of mutant hMre11 were obtained from ATLD LCLs from both families (Figures 6B and 6D). Accordingly, Western blotting of Nbs1 immunoprecipitates with hRad50 antiserum also showed that the indirect interaction between Nbs1 and hRad50 (via hMre11) was retained in all ATLD patients, albeit at a reduced level (Figures 6A and 6D). Immunoprecipitation with hMre11 and blotting with hRad50 revealed a strong interaction of the two in ATLD3 and ATLD4 (Figure 6C), but only a weak interaction in ATLD1 and ATLD2 (data not shown). In summary, it is clear that the stability of hMre11 protein interactions is compromised, but not abolished, by the ATLD mutations.

hRad50 (Figure 6D), but not hMre11, could be coimmunoprecipitated from the NBS cell line with Nbs1 antiserum. The inability to detect any coimmunoprecipitated hMre11 is likely to be a result of an interaction in this cell line beyond the detection limit of our assay. The *NSB1* mutations in this NBS cell line were 657del5 (the common Slavic mutation) and 698del4 in the second allele (Varon et al., 1998). Residual interaction of Nbs1 in other NBS cell lines is attributable to the presence of low levels of a variant Nbs1 protein that has been shown

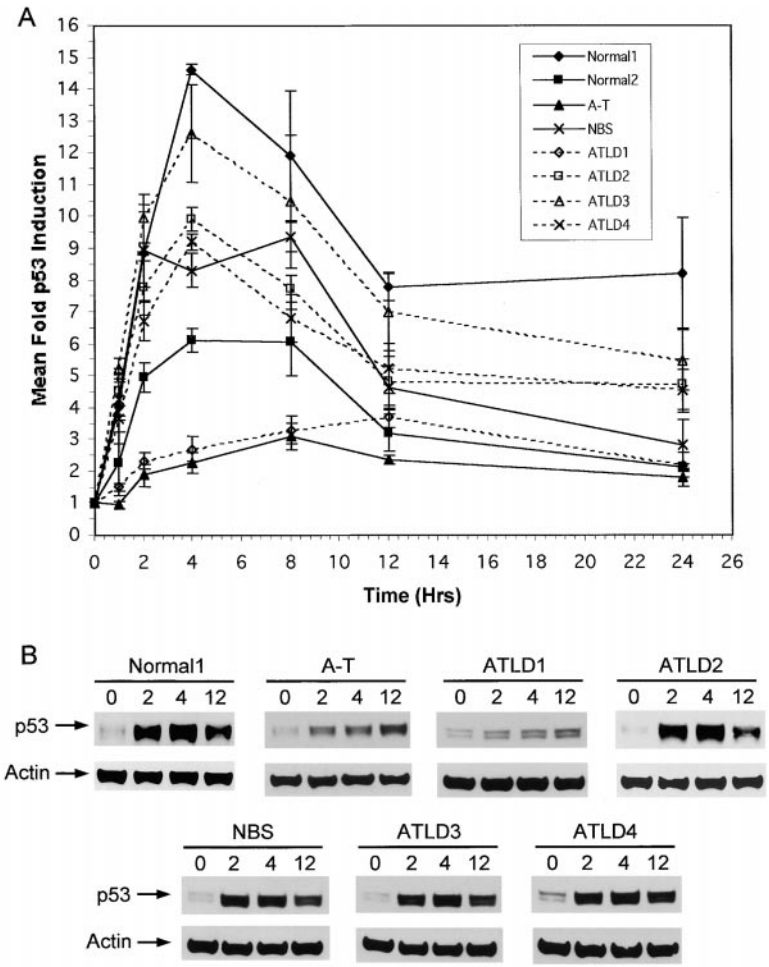

Figure 5. The p53 Response following Exposure of ATLD Cells to Ionizing Radiation Is Normal

(A) A graph showing the mean fold induction of p53 at different times after exposure of cells to 3 Gy ^{60}Co γ rays. The values are the means of three experiments for each cell line. (B) Western blots of p53 accumulation following exposure to ionizing radiation for 0, 2, 4, and 12 hr in the cell lines indicated. The Western blot was reprobed for actin to standardize for protein loading. The band density was quantified by densitometry to give data on fold increase in the graph above.

to retain the ability to interact with both hMre11 and hRad50 (R. S. M. et al., unpublished data).

Ionizing Radiation-Induced Foci of hMre11/hRad50/Nbs1 Complexes in ATLD Cells

Previous studies have shown that members of the hMre11/hRad50/Nbs1 protein complex become associated with DSBs early in the cellular DNA damage response (Nelms et al., 1998), and that these proteins form nuclear foci in response to IR and other DSB inducing agents (Maser et al., 1997; Carney et al., 1998). Ionizing radiation-induced foci (IRIF) formation is reduced in A-T cells, and this activity is abrogated in Nbs1-deficient fibroblasts (Maser et al., 1997; Carney et al., 1998). Given the phenotypic similarities among A-T, NBS, and ATLD cells, we examined IRIF formation in cell lines established from ATLD patients. ATLD2, 3, and 4 fibroblast cell lines were grown on glass slides, γ irradiated at a dose of 12 Gy, and stained with hMre11, Nbs1, or hRad51 antisera 3, 8, and 24 hr later. IRIF were subsequently visualized by immunofluorescence.

As observed previously in NBS cells (Carney et al., 1998), the subcellular distribution of the hMre11/hRad50/Nbs1 protein complex is aberrant in ATLD cells, irrespective of prior γ irradiation. Whereas hMre11 and Nbs1 immunoreactivity is exclusively nuclear in wild-type cells, hMre11 and Nbs1 staining is much more diffuse in the ATLD cells (Figures 7A, 7B, 7F, 7G, 7K, and 7L). The formation of Rad51 foci in the ATLD fibroblast cell lines was indistinguishable from that in IMR90 (normal) control fibroblasts. We have also shown that Rad51 IRIF form normally in NBS cells (unpublished data). These observations are consistent with the idea that Rad51 function is distinct from hMre11/hRad50/Nbs1 protein complex members in the cellular response to DSBs (Maser et al., 1997; Haber, 1998). The IMR90 control line exhibited 84% and 74% positive nuclei for Nbs1 and hMre11 IRIF, respectively, at 8 hr post γ irradiation, whereas fewer than 3% of nuclei contained IRIF at any time point in the ATLD cell lines (at least 100 nuclei were examined at each time point). The small number of hMre11 and Nbs1 IRIF detected in ATLD cells was aberrantly small and dull (e.g., Figure 7N). Thus, the IRIF response of ATLD cells expressing these mutant *hMRE11* alleles was essentially abrogated.

Discussion

Presented in this manuscript is the finding that a disorder, virtually indistinguishable from A-T, is caused by mutation in the *hMRE11* gene. Since the *hMRE11* locus is situated at 11q21 (Petrini et al., 1995) and the *ATM* locus at 11q23 (Gatti et al., 1988), only a very detailed linkage analysis would separate ATLD from A-T purely

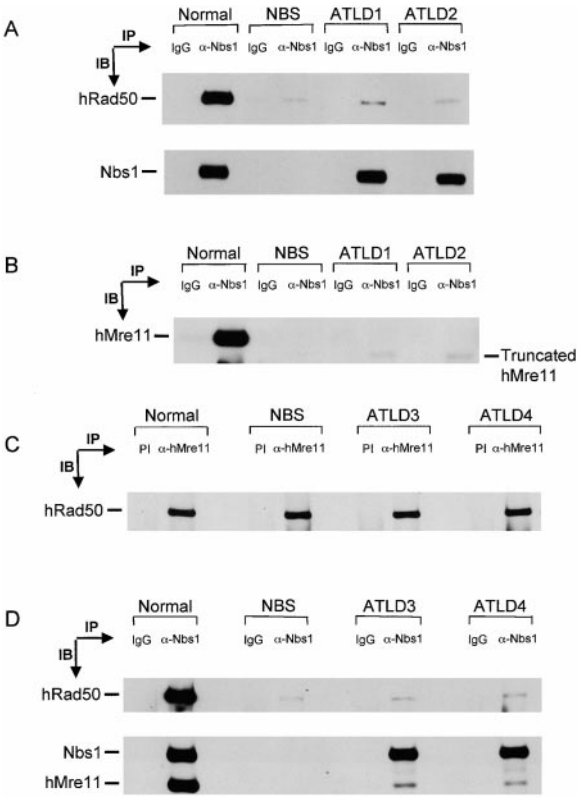

Figure 6. Interactions of Truncated or Mutant hMre11 Protein with hRad50 and Nbs1

Immunoprecipitation was carried out with either Nbs1 or hMre11 antisera using extracts of cells derived from ATLD1, 2, 3, and 4 and then subjected to Western blot analysis. The Western blots were probed with hRad50, Nbs1, or hMre11 antisera.

(A) Immunoprecipitation was carried out with an Nbs1 monoclonal antibody using cell extracts from a normal, NBS, and ATLD1 and 2 LCLs and blotted with hRad50. The amounts of lysate used for immunoprecipitation from ATLD cells were increased to compensate for lower levels of expression of hMre11/hRad50/Nbs1. The presence of equal amounts of immunoprecipitated Nbs1 was verified by reprobing the Western blot with antiserum directed against the Nbs1 protein (IgG; denotes immunoprecipitates using a nonspecific mouse IgG as a control).

(B) The same gel as in (A) was reprobed with hMre11 antiserum.

(C) Immunoprecipitation was carried out with anti-hMre11 antiserum using extracts of normal, NBS, and ATLD3 and 4 LCLs and blotted with hRad50 (PI denotes immunoprecipitates performed using the preimmune serum as a control).

(D) Immunoprecipitation was carried out with Nbs1 monoclonal antibody using normal, NBS, and ATLD3 and ATLD4 LCL extracts and blotted with hRad50 and hMre11. The presence of equal amounts of immunoprecipitated Nbs1 was again confirmed by subsequent reprobing with anti-Nbs1 antiserum.

on the basis of genetic data. Hence, molecular characterisations of the nature presented here may be required to distinguish the actual number of *hMRE11* mutants that present clinically with A-T. Assuming that the mutation rate is proportional to the length of the coding sequence of the two genes, ~6% of A-T cases might be expected to have *hMRE11* mutations.

Deficiency in Nbs1, a member of the protein complex in which hMre11 functions, forms the basis of a phenotypically similar chromosome instability syndrome, NBS (Carney et al., 1998). Although the clinical phenotypes of A-T and NBS are quite distinct, the similarity between NBS and A-T at the cellular level is striking. Cells derived from A-T and NBS patients are unusually sensitive to the killing effects of ionizing radiation, show increased levels of chromosome translocations, and fail to activate specific cell cycle checkpoints in response to DNA damage (Shiloh, 1997).

The finding reported here that mutation of hMre11, a second hMre11/hRad50/Nbs1 protein complex member, leads to both the clinical and cellular phenotypes of A-T provides compelling evidence that this complex acts in the same pathway as ATM. The data demonstrate that ATM and members of the hMre11/hRad50/Nbs1 protein complex are not functionally redundant. Of particular note is the observation of radioresistant DNA synthesis in A-T, NBS, and ATLD, a phenotypic feature that is unique to these three chromosome instability syndromes. This phenotypic outcome indicates that a significant component of S phase DNA damage recognition and checkpoint activation is dependent upon the DNA damage response pathway defined by hMre11/hRad50/Nbs1 and ATM.

In addition to the regulation of the S phase checkpoint, the data presented argue that other underlying mechanistic defects in A-T, ATLD, and NBS overlap to a significant extent. For example, it has been shown that A-T cells are deficient in the activation of c-Jun N-terminal kinase (JNK) following exposure to IR (Shafman et al., 1995). The abnormal response in A-T cells is due to a specific requirement for functional ATM and c-Abl for the activation of JNK. The activation of JNK after exposure to IR was found to be defective in all four ATLD cell lines as well as in the NBS cell line and comparable to that exhibited by classical A-T cells.

On the other hand, ATM clearly participates in parallel, independent stress responses. In particular, the p53 response in A-T cells differs markedly from that in NBS or ATLD cells. Whereas the ATM deficiency results in an impaired ability of the cell to accumulate p53 following exposure to ionizing radiation (Kastan et al., 1992), the p53 response was found to be normal in three of the four affected ATLD patients as well as in the NBS cell line examined here. In this regard, ATLD cells more closely resemble NBS cells that do not tend to show such a pronounced p53 defect (Khanna and Lavin, 1993; Yamazaki et al., 1998). It can therefore be inferred that there is a specific requirement for a functional hMre11/hRad50/Nbs1 complex in selected ATM-dependent stress response pathways, whereas other pathways, such as that which leads to induction of p53, are independent parallel pathways. Given the clinical and cellular similarities between A-T and ATLD, this finding also implies that the defective p53 response may play a minor role in the development of the A-T phenotypes.

The mechanistic basis for the ATLD phenotypes is clearly of great interest. The *hMRE11* mutations described do not lead to gross deficiency in DSB repair; a similar observation has been made in NBS cells (Nove et al., 1986; Kraakman-van der Zwet et al., 1999). These alleles may define a function, or class of functions, of the hMre11/hRad50/Nbs1 protein complex that is separable from its role in recombinational DNA repair. Alternatively, the mechanisms of the complex's action in effecting

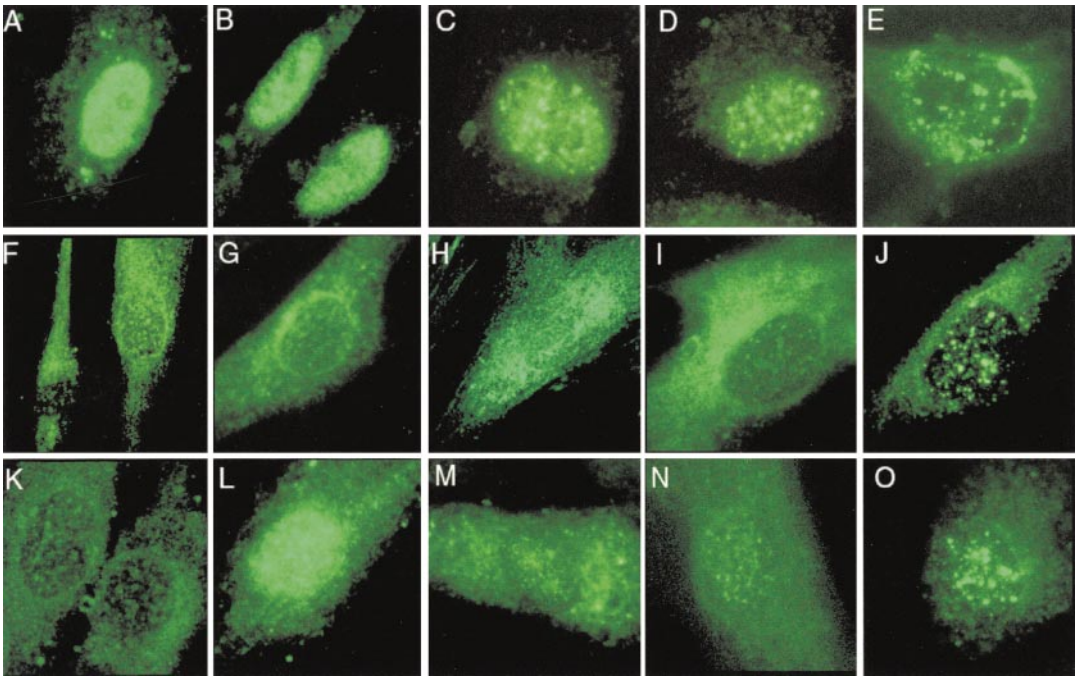

Figure 7. IRIF Formation in ATLD Fibroblasts

IMR90 (A–E), ATLD2 (F–J), ATLD3 and 4 (K–O) fibroblast cell lines were γ irradiated at 12 Gy and fixed 8 hr post irradiation. Cells were stained for immunofluorescence with Nbs1, hMre11, and Rad51 polyclonal antisera as described in Experimental Procedures. Unirradiated controls stained with hMre11 antiserum (A, F, and K) and Nbs1 antiserum (B, G, and L) are compared with irradiated samples stained with hMre11 (C, H, and M), Nbs1 (D, I, and N), and Rad51 antisera (E, J, and O). Cells stained with hMre11 and Nbs1 were costained with Ku86 mAb to control for nuclear integrity.

DNA repair and in activating cell cycle checkpoint functions may be similar. In this scenario, overt DNA repair deficiency would only be detectable in null or profoundly hypomorphic mutants, whereas cell cycle checkpoint defects would be the primary manifestation of mildly hypomorphic mutants.

The Effect of *hMRE11* Mutations on hMre11/hRad50/Nbs1 Complex Formation

Attempts to create null mutants of *mMRE11* and *mRAD50* have resulted in lethality, indicating that the complex mediates essential functions (Xiao and Weaver, 1997; Luo et al., 1999). Consistent with the essential nature of the complex, Carney et al., (1998) showed that hMre11/hRad50 complexes form in cells derived from NBS patients. *hMRE11* alleles are not null in the ATLD patients, and both the truncated and full-length (N117S) mutant hMre11 proteins retain the ability to associate with hRad50 as well as Nbs1. It could, therefore, be inferred that the effects of the two *hMRE11* gene mutations on the hMre11/hRad50/Nbs1 complex are subtle, affecting the efficiency of protein binding, rather than completely abrogating it, and thereby maintaining cell viability.

The missense mutation (N117S) in cells from ATLD patients 3 and 4 selectively affects Nbs1, but not hRad50, binding. This may suggest that the Nbs1-binding site is located within the N-terminal portion of the human hMre11 protein. This region of Mre11 is likely to be important for the coordination of a divalent cation (Zhuo et al., 1993, 1994; Sharples and Leach, 1995). Mutations in this region that impair metal binding may exert a global impact on Mre11 structure and in turn influence molecular interactions at distal sites on the hMre11 protein.

Interestingly, the *hMRE11* mutations present in all four ATLD patients results in reduced levels of both hRad50 and Nbs1 proteins. The most plausible explanation for this is that alteration in one member of a multiprotein complex can destabilize some or all of its protein components.

Irradiation-Induced hMre11 and Nbs1 Foci

We found that the formation of IRIF of hMre11 and Nbs1 was essentially abrogated in ATLD fibroblasts. Using a technique in which discrete subnuclear volumes are damaged by ionizing radiation, it has been established that the hMre11/hRad50/Nbs1 protein complex associates with damaged DNA (Nelms et al., 1998). The bulk of evidence suggests that IRIF formation reflects the association of the complex with DNA damage, and that the emergence of IRIF relatively long after IR treatment reflects the presence of slowly repaired or irreparable lesions (Cornforth and Bedford, 1983; Nevaldine et al., 1993). Therefore, the coincidence of aberrant IRIF formation and deficiency in the activation of DNA damage responses provides further support for the hMre11/hRad50/Nbs1 protein complex as a sensor of DNA damage that is critical for activation of cell cycle checkpoint functions mediated by ATM.

The hMre11/hRad50/Nbs1 Complex: Functional Link to ATM

The importance of Nbs1 and ATM in the maintenance of genomic stability is well established. A-T patients showing either loss of ATM or the presence of some mutant ATM have an increased risk of developing lymphoid tumors (Taylor et al., 1996b). Disruption of the hMre11/hRad50Nbs1 complex through mutations in the *NBS1* gene in patients with NBS also results in a high frequency of lymphoma in these individuals (Carney et al., 1998; Varon et al., 1998). Although the role of inherited and acquired *hMRE11* mutations in the development of tumors is currently unknown, disruption of the hMre11/hRad50/Nbs1 complex through mutations in the *hMRE11* gene is also likely to be associated with an increased risk of lymphoid tumor development. This question can be directly addressed through the derivation of murine models for ATLD. Clearly, disruption of the DNA damage response pathway in which these proteins function leads to decreased genome stability and strongly potentiates the onset and progression of malignancy.

Experimental Procedures

ATLD Patients

Patients ATLD1 and ATLD2 were first cousins and part of a large inbred family from Pakistan. Both had progressive cerebellar degeneration (clinical details are given in Hernandez et al. [1993]). The seven siblings and mother of ATLD1 were normal (father is deceased). The parents of ATLD2 were also first cousins in this family, and the father of ATLD2 and mother of ATLD1 were siblings. The remaining siblings and parents of ATLD2 were normal (Hernandez et al., 1993). Neither patient ATLD1 nor ATLD2 showed any intellectual inpairment. Serum immunoglobulins and AFP levels were also normal in both patients.

In the second family, two of three sons (ATLD3 and ATLD4), born to nonconsanguineous parents, developed features of ataxia-telangiectasia, including progressive cerebellar degeneration. The older brother appeared to have more severe features (for further details of this family, see Klein et al. [1996]).

None of these ATLD patients showed any evidence of immune deficiency or any cancer.

Cells

Lymphoblastoid cell lines (LCLs) and skin fibroblast strains were derived from normal individuals and patients with A-T and NBS using methods previously described. LCLs were derived for ATLD patients 1–4, and five of the six parents and were routinely maintained in RPMI medium supplemented with 10% FCS, glutamine and penicillin and streptomycin. Skin fibroblast strains were grown from patients ATLD1–4 and were maintained in Dulbecco's Modified Eagles Medium with the same supplements.

Colony Forming Ability following γ Ray Exposure

Different dilutions of skin fibroblasts were irradiated with doses of γ rays between 1.0 and 5.0 Gy and seeded on to lethally irradiated feeder layers of the same cells (6×10^4 per 9 cm dish irradiated with 35 Gy γ rays). Cells were left for 14–21 days in an incubator to form colonies with a change of medium once per week, stained with methylene blue, and counted.

Radioresistant DNA Synthesis Assay

One day after seeding into multiple 3 cm dishes ($4–8 \times 10^4$ per dish), primary fibroblasts were prelabelled for 16 hr with [2-^{14}C]-thymidine (50 nCi/ml, 50 μCi/mmol), exposed to graded doses of Cs-γ rays (about 1 Gy/min) at room temperature, and subsequently labeled with [*methyl*-^{3}H]-thymidine (2 μCi/ml, 2 Ci/mmol) for 4 hr. Cultures were rinsed with phosphate-buffered saline, lysed in 0.5 ml 0.25M NaOH, and transferred to 7.5 ml Soluene counting fluid (Packard) for liquid scintillation counting using a dual-label program (Kleijer et al., 1994). DNA synthesis was estimated by ^{3}H/^{14}C dpm ratios and expressed as a percentage of unirradiated controls.

Pulsed-Field Gel Electrophoresis

Cells were labeled with 0.05 μCi/ml [^{14}C]-thymidine (54 mCi/mmol)for 2 days prior to irradiation. Cells were iced (~10 min) and either irradiated on ice at 50 Gy in a Mark I ^{137}Cs source (~3 Gy/min) or mock irradiated. Cells were warmed briefly in a 37°C water bath before being incubated for 0, 45, or 90 min. 500 μl ($\sim 5 \times 10^5$) cells were pelleted, warmed briefly at 50°C, resuspended in 90 μl of 1% low melting point agarose (GIBCO–BRL) in buffer L (10 mM Tris, 20 mM NaCl, 100 mM EDTA [pH 8.0]). Cells were immediately pipetted into plug molds (BioRad) and placed at 4°C.

Solidified plugs were incubated at 50°C for 24 hr in 0.6 ml of lysis solution (0.85× buffer L, 1% sarkosyl, 1 mg/ml Proteinase K), then washed twice in TE (10 mM Tris, 100 mM EDTA [pH 8.0]) and stored at 4°C. Pulsed-field gel electrophoresis was performed using a CHEF-DR III apparatus (BioRad) essentially as described (Rydberg et al., 1994). Gels were 0.75% agarose (GIBCO–BRL) in 0.5× LRTBE (135 mM Tris base, 45 mM Boric acid, 7.5 mM EDTA). About one-third of a plug was loaded per well, and *S. cerevisiae* chromosomes (BioRad) were loaded as size standards. 1% low-melting point agarose in TE was subsequently added to immobilize the plugs within the wells. Gels were run in 0.5× LRTBE at 14°C at 50 V (1.5 V/cm) with a switch time linearly changing from 1 hr to 1 min over 68 hr. After electrophoresis, gels were stained in a 1:10000 dilution of Vistra Green (Amersham) and scanned using a Storm 860 PhosphorImager (Molecular Dynamics).

The portion of each lane that contained either the plug or DNA that entered the gel in an irradiation-dependent manner was sliced into 0.5 cm-wide sections. Each gel slice was transferred to a liquid scintillation vial containing 0.1 ml 1 M HCl, warmed on a hot plate to hydrolyze the agarose, and neutralized with 0.1 ml 1 M NaOH. Scintisafe Econo2 (Fisher) (5 ml) was added to each vial, and samples were counted for 10 min on a Tri-Carb liquid scintillation analyzer (Packard). The fraction of activity released (FAR) was calculated as (^{14}C that entered the gel)/(^{14}C in plug + ^{14}C that entered the gel), and FAR_{IR} = FAR (irradiated cells) − FAR (controls).

p53 Induction Assay

Exponentially growing LCLs ($\sim 4 \times 10^6$ per time point) were irradiated with 3 Gy of ^{60}Co γ rays (~1 Gy/min) and subsequently incubated at 37°C. Cells were harvested at the time points indicated and whole-cell extracts made (see above). Twenty micrograms of whole-cell extract from each time point was routinely loaded onto a 10% SDS-polyacrylamide gel and analyzed by immunoblotting. To verify protein equal loading, the filters were additionally probed with an anti-Actin monoclonal antibody (AC74). Band density was quantified using scanning densitometry.

c-Jun N-Terminal Kinase Assay

LCLs ($\sim 4 \times 10^7$) were irradiated with 20 Gy of ^{60}Co γ rays (about 2 Gy/min) at room temperature and subsequently incubated for 1 hr at 37°C. The cells were resuspended in lysis buffer (20 mM Tris/HCl [pH 7.6], 0.5% [v/v] Triton X-100, 250 mM NaCl, 3 mM EGTA, 3 mM EDTA, 200 μM phenylmethylsulfonyl fluoride [PMSF], 2 mM sodium orthovanadate, 10 μg/ml aprotinin, 10 μg/ml leupeptin, 1 mM dithiothreitol [DTT], 50 mM NaF) and incubated for 45 min. Two hundred fifty micrograms of whole-cell extract was used per immunoprecipitation. Rabbit anti-JNK antibody (0.5 μg) (Santa Cruz sc-474) or equivalent amount of nonspecific rabbit IgG (Sigma) was added to each immunoprecipitation and then incubated for 2 hr at 4°C. Bead-bound immunoprecipitates were washed once with lysis buffer and then twice with kinase buffer (20 mM HEPES [pH 7.5], 20 mM β-glycerophosphate, 10 mM $MgCl_2$, 10 mM $MnCl_2$, 1 mM DTT, 50 μM sodium orthovanadate). Each immunoprecipitate was resuspended in 30 μl of kinase buffer supplemented with 1 μM cold ATP (Sigma), 2 μg of GST-c-Jun (Stratagene), and 1 μCi ^{32}P-γ-ATP (10 mCi/ml, 3000 Ci/mmol) (Amersham) and incubated at 30°C for 30 min. The kinase reaction was stopped by the addition of SDS sample buffer and boiled for 5 min. Proteins were fractionated on a 12% SDS-polyacrylamide gel. Proteins were visualized by silver staining, and the gel was dried and then subjected to autoradiography.

Immunoblot Analysis

Whole-cell extracts (from ~4 × 10^6 cells) were prepared as described (Stankovic et al., 1999). Briefly, cells were sonicated in UTB buffer (9 M Urea, 150 mM β-mercaptoethanol, 50 mM Tris/HCl [pH7.5]) and cellular debris removed by centrifugation. Proteins were fractionated in 6% SDS-polyacrylamide gels. Proteins were transferred to nitrocellulose, and immunoblots were performed with p53 (donated by D. P. Lane), ATM (FP8r) (Stankovic et al., 1998), hMre11, Nbs1, and hRad50 (Dolganov et al., 1996; Carney et al., 1998) antisera. To verify that equivalent amounts of each sample were loaded, the filters were additionally probed with an actin monoclonal antibody (AC74, Sigma). Band density was quantified using scanning densitometry.

Immunoprecipitation

LCLs (~4× 10^7) were lysed on ice for 30 min in lysis buffer (10 mM Tris/HCl [pH 7.5], 100 mM NaCl, 5 mM EDTA, 0.5% Nonidet P-40, 0.5 mM PMSF, 2 mM sodium orthovanadate, 10 μg/ml leupeptin). Precleared lysates were incubated on ice for 1 hr with hMre11 antiserum (204/3p), hMre11 preimmune serum (204pre), Nbs1 monoclonal antibody 9H4 ascites fluid, or nonspecific mouse IgG. Immune complexes were precipitated for 1–2 hr by rolling at 4°C with protein A-agarose or agarose-coupled anti-mouse IgG beads. Immunoprecipitates were washed four times with lysis buffer, boiled in SDS sample buffer, and loaded on SDS 6% polyacrylamide gels. Proteins were analyzed by immunoblotting using standard methods and detected as described above.

Mutation Analysis

Mutation analysis of the *ATM* gene was performed by RT–PCR and restriction endonuclease fingerprinting (REF) using cDNA prepared from lymphoblastoid cell lines of individual patients (Byrd et al. 1996).

Mutation analysis of the genes *TP53* and *hMRE11* was performed by RT–PCR and sequencing of the entire coding region.

Yeast Irradiation Studies

Radiation sensitivity of *Scmre11* mutants was examined in transformants of the haploid *Scmre11*Δ strain JPY180 (*MAT* **a** *his7 leu2 ura3 trp1 mre11::hisG*). Construction of the TRP-marked centromeric *ScMRE11* expression construct pScM11–314 has been described elsewhere (Bressan et al., 1999). Site-specific mutations in *MRE11* were generated by linear amplification using complementary 35-mer primers. Restriction fragments bearing the desired mutation(s) were confirmed by DNA sequencing. Yeast media and strain manipulations were carried out according to standard procedures (Ausubel et al., 1989; Guthrie and Fink, 1991).

Yeast strains were γ irradiated in mid-log phase (~1 × 10^7 cells/ml) using a Mark I ^{137}Cs source at a dose rate of 3 Gy/min. Cells were plated on to SC-trp media, incubated at 30°C, and scored for colony formation for 5 days following irradiation.

Assaying for Ionizing Radiation-Induced Foci

Immunofluorescence on primary human fibroblasts was performed as described in Maser et al. (1997) and Carney et al. (1998). Briefly, cells were mock treated or irradiated with 12 Gy and fixed 8 hr postirradiation in methanol, followed by permeabilization with acetone. Cells were blocked for 30 min in 10% FCS in PBS, followed by incubations for 45 min at room temperature with primary antibodies diluted in 1% BSA in PBS. Following three washes with PBS, cells were incubated for 30 min with FITC-conjugated anti-rabbit and Texas red–conjugated anti-mouse antibodies, diluted in 1% BSA in PBS. Cells were then washed three times with PBS, followed by counterstaining for 1 min with 0.1 μg/ml DAPI. Antifade solution (2.3% DABCO, 0.1 M Tris-HCl [pH 8], 90% glycerol) was applied to the slides, and coverslips were mounted. Cells were viewed using a 60× oil immersion objective. Images were recorded, pseudo-colored, and merged as previously described (Carney et al., 1998).

Antisera

Antiserum against the full-length hMre11 protein was generated using full-length hMre11 fused to GST as an antigen in New Zealand white rabbits. Nbs1 monoclonal antibody 9H4 was raised against full-length human Nbs1 fused to glutathione S-transferase (GST). All other antisera were generated and used as previously described (Maser et al., 1997; Carney et al., 1998). The anti-Ku86 monoclonal antibody (N3H10) was a gift from R. Burgess (University of Wisconsin, Madison), and Rad51 antiserum was a gift from A. Shinohara.

Acknowledgments

G. S. was supported by a PhD studentship funded by the Ataxia Telangiectasia Society of the U. K. We also thank the Cancer Research Campaign, the Kay Kendall Leukaemia Fund, and the Wellcome Trust for their continued support. J. H. J. P., R. S. M., D. A. B., and M. I. K. are supported by NIH/NCI GM56888, GM59413, and the Milwaukee Foundation. We thank Richard Burgess and Akira Shinohara for immunological reagents.

Received August 24, 1999; revised November 19, 1999.

References

Ager, D.D., and Dewey, W.C. (1990). Calibration of pulsed field gel electrophoresis for measurement of DNA double-strand breaks. Int. J. Radiat. Biol. *58*, 249–259.

Ajimura, M., Leem, S.H., and Ogawa, H. (1993). Identification of new genes required for meiotic recombination in *Saccharomyces cerevisiae*. Genetics *133*, 51–66.

Ausubel, F.M., Brent, R., Kingston, R.E., Moore, D.D., Seidman, J.G., et al., (1989). Current Protocols in Molecular Biology (New York: John Wiley and Sons).

Bressan, D.A., Olivares, H.A., Nelms B.E., and Petrini, J.H. (1998). Alteration of N-terminal phosphoesterase signature motifs inactivates *Saccharomyces cerevisiae* Mre11. Genetics *150*, 591–600.

Bressan, D.A., Baxter, B.K., and Petrini, J.H.J. (1999). The Mre11/Rad50/Xrs2 protein complex facilitates homologous recombination-based double strand break repair in *Saccharomyces cerevisiae*. Mol. Cell. Biol., in press.

Byrd, P.J., Cooper, P., Stankovic, T., Kullar, H.S., Watts, G.D.J., Robinson, P.J., and Taylor, A.M.R. (1996). A gene transcribed from the bidirectional ATM promoter coding for a serine rich protein: amino acid sequence, structure and expression. Hum. Mol. Genet. *5*, 1785–1791.

Carney, J.P., Maser, R.S., Olivares, H., Davis, E.M., Le Beau, M., Yates, J.R., Hays, L., Morgan, W.F., and Petrini, J.H.J. (1998). The hMre11/hRad50 protein complex and Nijmegen breakage syndrome: linkage of double-strand-break repair to the cellular DNA damage response. Cell *93*, 477–486.

Cornforth, M.N., and Bedford, J.S. (1983). X-ray-induced breakage and rejoining of human interphase chromosomes. Science *222*, 1141–1143.

Dolganov, G.M., Maser, R.S., Novikov, A., Tosto, L., Chong, S., Bressan, D.A., and Petrini, J.H.J. (1996). Human Rad50 is physically associated with human Mre11: identification of a conserved multiprotein complex implicated in recombinational DNA repair. Mol. Cell. Biol. *16*, 4832–4841.

Furuse, M., Nagase, Y., Tsubouchi, H., Murakami-Murofushi, K., Shibata, T., and Ohta, K. (1998). Distinct roles of two separable in vitro activities of yeast mre11 in mitotic and meiotic recombination. EMBO J. *17*, 6412–6425.

Gatti, R.A., Berkel, I., Boder, E., Braedt, G., Charmley, P., Concannon, P., Ersoy, F., Foroud, T., Jaspers, N.G., Lange, K., et al. (1988). Localization of an ataxia-telangiectasia gene to chromosome 11q22–23. Nature *336*, 577–580.

Guthrie, C., and Fink, G.R., eds. (1991). Guide to yeast genetics and molecular biology. Methods Enzymol. *194*, 1–863.

Haber, J.E. (1998). The many interfaces of Mre11. Cell *95*, 583–586.

Hernandez, D., McConville, C.M., Stacey, M., Woods, C.G., Brown, M.M., Shutt P, Rysiecki, G., and Taylor, A.M.R. (1993). A family showing no evidence of linkage between the ataxia telangiectasia gene and chromosome 11q22–23. J. Med. Genet. *30*, 135–140.

Jaspers, N.G.J., de Wit, J., Regulski, M.R., and Bootsma, D. (1982).

Abnormal regulation of DNA replication and increased lethality in ataxia telangiectasia cells exposed to carcinogenic agents. Cancer Res. *42*, 335–341.

Jorgensen, T.J., and Shiloh, Y. (1996). The ATM gene and the radiobiology of ataxia-telangiectasia. Int. J. Radiat. Biol. *69*, 527–537.

Kastan, M.B., Zhan, Q., El Deiry, W.S., Carrier, F., Jacks, T., Walsch, W.V., Plunkett, B.S., Vogelstein, B., and Fornace, A.J., Jr. (1992). A mammalian cell cycle checkpoint pathway utiliizing p53, and Gadd45 is defective in ataxia-telangiectasia. Cell *71*, 587–597.

Khanna, K.K., and Lavin, M.F. (1993). Ionising radiation and UV induction of p53 protein by different pathways in ataxia-telangiectasia cells. Oncogene *8*, 3307–3312.

Kleijer, W.J., van der Kraan, M., Los, F.J., and Jaspers, N.G.J. (1994). Prenatal diagnosis of ataxia telangiectasia and Nijmegen Breakage Syndrome by the assay of radioresistant DNA synthesis. Int. J. Radiat. Biol. *66*, S167–S174.

Klein, C., Wenning, G.K., Quinn, N.P., and Marsden, C.D. (1996). Ataxia without telangiectasia masquerading as benign hereditary chorea. Mov. Disord. *11*, 217–220.

Kraakman-van der Zwet, M., Overkamp, W.J., Friedl, A.A., Klein, B., Verhaegh, G.W., Jaspers, N.G., Midro, A.T., Eckardt-Schupp, F., Lohman, P.H., and Zdzienicka, M.Z. (1999). Immortalization and characterization of Nijmegen breakage syndrome fibroblasts. Mutat. Res. *434*, 17–27.

Lees-Miller, S.P., Godbout, R., Chan, D.W., Weinfeld, M., Day, R.S., III, Barron, G.M., and Allalunis-Turner, J. (1995). Absence of p350 subunit of DNA-activated protein kinase from a radiosensitive human cell line. Science *267*, 1183–1185.

Luo, G., Yao, M.S., Bender, C.F., Mills, M., Bladl, A.R., Bradley, A., and Petrini, J.H.J. (1999). Disruption of mRad50 causes embryonic stem cell lethality, abnormal embryonic development, and sensitivity to ionising radiation. Proc. Natl. Acad. Sci. USA *96*, 7376–7381.

Maser, R.S., Monsen, K.J., Nelms, B.E., and Petrini, J.H.J. (1997). hMre11 and hRad50 nuclear foci are induced during the normal cellular response to DNA double-strand breaks. Mol. Cell Biol. *17*, 6087–6096.

McConville, C.M., Stankovic, T., Byrd, P.J., McGuire, G., Yao, Q-Y., Lennox, G.G., and Taylor, A.M.R. (1996). Mutations associated with variant phenotypes in ataxia telangiectasia. Am. J. Hum. Genet. *59*, 320–330.

Nairz, K., and Klein, F. (1997). mre11S—a yeast mutation that blocks double-strand-break processing and permits nonhomologous synapsis in meiosis. Genes Dev. *11*, 2272–2290.

Nelms, B.E., Maser, R.S., MacKay, J.F., Lagally, M.G., and Petrini, J.H. (1998). In situ visualization of DNA double-strand break repair in human fibroblasts. Science *280*, 590–592.

Nevaldine, B., Longo, J.A., King, G.A., Vilenchik, M., Sagerman, R.H., and Hahn, P.J. (1993). Induction and repair of DNA double-strand breaks. Radiat. Res. *133*, 370–374.

Nove, J., Little, J.B., Mayer, P.J., Troilo, P., and Nichols, W.W. (1986). Hypersensitivity of cells from a new chromosomal-breakage syndrome to DNA-damaging agents. Mutat. Res. *163*, 255–262.

Petrini, J.H.J., Walsh, M.E., Di Mare, C., Korenberg, J.R., Chen, X.-N., and Weaver, D.T. (1995). Isolation and characterization of the human MRE11 homologue. Genomics *29*, 80–86.

Petrini, J.H., Bressan, D.A., and Yao, M.S. (1997). The RAD52 epistasis group in mammalian double strand break repair. Semin. Immunol. *9*, 181–188.

Rydberg, B., Löbrich, M., and Cooper, P.K. (1994). DNA double-strand breaks induced by high-energy neon and iron ions in human fibroblasts. I. Pulsed-field gel electrophoresis method. Radiat. Res. *139*, 133–141.

Savitsky. K., Bar-Shira, A., Gilad, S., Rotman, G., Ziv, Y., Vanagaite, L., Tagle, D.A., Smith, S., Uziel, T., Sfez, S., et al. (1995). A single ataxia telangiectasia gene with a product similar to PI-3 kinase. Science *268*, 1749–1753.

Shafman, T.D., Saleem, A., Kyriakis, J., Weichselbaum, R., Kharbanda, S., and Kufe, D.W. (1995). Defective induction of stress-activated protein kinase activity in ataxia telangiectasia cells exposed to ionizing radiation. Cancer Res. *55*, 3242–3245.

Sharples, G.J., and Leach, D.R. (1995). Structural and functional similarities between the SbcCD proteins of Escherichia coli and the RAD50 and MRE11 (RAD32) recombination and repair proteins of yeast. Mol. Microbiol. *17*, 1215–1217.

Shiloh, Y. (1997). Ataxia-telangiectasia and the Nijmegen breakage syndrome: related disorders but genes apart. Annu. Rev. Genet. *31*, 635–662.

Stankovic, T., Kidd, A.M.J., Sutcliffe, A., McGuire, G.M., Robinson, P., Weber, P., Bedenham, T., Easton, D.F., Lennox, G.G., Haites, N., Byrd, P.J., and Taylor, A.M.R. (1998). ATM mutations and phenotypes in A-T families in the British Isles: expression of mutant ATM and the risk of leukaemia, lymphoma and breast cancer. Am. J. Hum. Genet. *62*, 334–345.

Stankovic, T., Weber, P., Stewart, G., Bedenham, T., Murray, J., Byrd, P.J., Moss, P.A.H., and Taylor, A.M.R. (1999). The ataxia telangiectasia mutated (ATM) gene is frequently inactivated in B cell chronic lymphocytic leukaemia. Lancet *353*, 26–29.

Taylor, A.M.R., Hernandez, D., McConville, C.M., Woods, C.G., Stacey, M., Biggs, P., Byrd, P.J., Arlett, C.F., and Scott, D. (1996a). Malignant disease and variations in radiosensitivity in ataxia telangiectasia patients. In Genetic Predisposition to Cancer. R.A. Eeles, B.A.J. Ponder, D.F. Easton, and D. Horwich, eds. (London: Chapman and Hall), pp. 138–151

Taylor, A.M.R., Metcalfe, J.A., Thick, J., and Mak, Y-F. (1996b). Leukaemia and lymphoma in ataxia telangiectasia. Blood *87*, 423–438.

Usui, T., Ohta, T., Oshiumi, H., Tomizawa, J., Ogawa, H., and Ogawa T. (1998). Complex formation and functional versatility of Mre11 of budding yeast in recombination. Cell *95*, 705–716.

Varon, R., Vissinga, C., Platzer, M., Cerosaletti, K.M., Chrzanowska, K.H., Saar, K., Beckmann, G., Seemanova, E., Cooper, P.R., Nowak, N.J., et al. (1998). Nibrin, a novel DNA double-strand break repair protein, is mutated in Nijmegen breakage syndrome. Cell *93*, 467–476.

Xiao, Y., and Weaver, D.T. (1997). Conditional gene targeted deletion by Cre recombinase demonstrates the requirement for the double-strand break repair Mre11 protein in murine embryonic stem cells. Nucleic Acids Res. *25*, 2985–2991.

Yamazaki, V., Wegner, R.-D., and Kirchgessner, C.U. (1998). Characterisation of cell cycle checkpoint responses after ionising radiation in Nijmegen Breakage Syndrome cells. Cancer Res. *58*, 2316–2322.

Zhuo, S., Clemens, J.C., Hakes, D.J., Barford, D., and Dixon, J.E. (1993). Expression, purification, crystallization, and biochemical characterization of a recombinant protein phosphatase. J. Biol. Chem. *268*, 17754–17761.

Zhuo, S., Clemens, J.C., Stone, R.L., and Dixon, J.E. (1994). Mutational analysis of a Ser/Thr phosphatase. J. Biol. Chem. *269*, 26234–26238.